Heteroleptic copper(I)-polypyridine complexes as efficient sensitizers for dye sensitized solar cells

Martina Sandroni,[ac] Ludovic Favereau,[a] Aurelien Planchat,[a] Huriye Akdas-Kilig,[b] Nadine Szuwarski,[a] Yann Pellegrin,[a] Errol Blart,[a] Hubert Le Bozec,[b] Mohammed Boujtita*[a] and Fabrice Odobel*[a]

The synthesis and the physico-chemical characterizations of HETPHEN based heteroleptic copper(I)-bis(diimine) complexes are reported. In TiO_2 based dye sensitized solar cells (DSCs), the latter display impressive photoconversion efficiencies (PCEs), unprecedented for first row transition metal coordination complexes.

Since 1991[1] and the discovery of DSC (Grätzel cells), many attempts to replace the costly and toxic (albeit remarkably efficient) ruthenium-polypyridine complexes have been reported.[2, 3] Copper(I)-bis(diimine) complexes have early shown promising results in this field.[4, 5, 6] Lately, the use of heteroleptic copper(I) complexes has afforded significant PCEs thanks to an improved extinction coefficient in the visible and electron transfer vectorialization.[6] The latter point is an essential criterion to fulfil in the design of efficient sensitizers for TiO_2. Indeed, each ligand is set to play one (or more) well-defined role such as anchoring, passivation of the surface and assisting charge injection. Accordingly, ligands differ by their molecular structures and therefore by their electronic natures. In the course of our program on heteroleptic bis-diimine copper(I) complexes,[7, 8, 9] prepared according to the HETPHEN concept developed by Schmittel and colleagues,[10] we have prepared and studied four new stable heteroleptic copper(I) complexes $[CuL^0L^n]^+$ hereafter named **Cn** (n = 1-4, Figure 1).

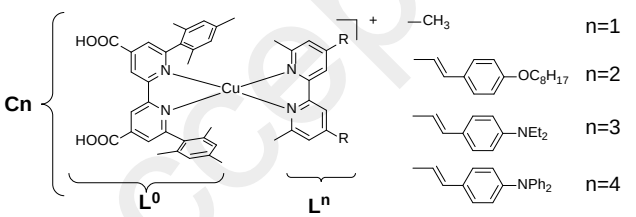

Figure 1. Molecular structures of $\mathbf{L^n}$ and **Cn** (n=1-4)

The anchoring ligand $\mathbf{L^0}$ (6,6'-dimesityl-2,2'-bipyridine-4,4'-dicarboxylic acid) is based on the classical 4,4'-dicarboxylic acid bipyridine onto which were attached two mesityl groups in positions 6 and 6', providing the necessary steric bulk to avoid the formation of homoleptic complexes. The ligands completing the coordination sphere of the copper(I) ion belong to the family of 4,4'-bis(styrylphenyl)-2,2'-bipyridines, derivatized with electron releasing moieties of different strength. Methyl groups in α of the chelating nitrogen atoms confer rigidity to the final scaffold, preserving the excited state from exciplex quenching and excessive flattening upon excitation, to a certain extent. Three complexes **C2**, **C3** and **C4**, bearing respectively alkoxy, N,N-diethylamine and N,N-diphenylamine moieties were thus isolated. For the sake of comparison, a fourth model complex $[CuL^0L^1]^+$ (**C1**) was synthesized, with L^1 = 2,2',4,4'-tetramethylbipyridine.

The syntheses of all ligands are reported in ESI. The HETPHEN *modus operandi* was used to isolate **C1-4** and started with the synthesis of the $Cu(\mathbf{L^0})]^+$ intermediate in DMF. An equivalent of L^n was subsequently added dropwise, entailing an immediate colour change of the medium from yellow to deep red. Impurities were removed by size exclusion chromatography. A similar protocol was used to isolate the dimethyl-ester forms of each complex (named hereafter **Cnester**, n=1-4, synthesis given in ESI).

The electronic absorption spectra of the complexes were recorded in solution and on nanocrytalline TiO_2 films (Figures 2 and S3). All the complexes featured the classical MLCT absorption band at ca. 500 nm (Table 1 and Figure 2).[11] The increased conjugation of the π system on both $\mathbf{L^0}$ and $\mathbf{L^n}$ (n = 2-4) induces a stabilization of the π* orbitals, explaining the red-shift of this transition compared to the benchmark bis-neocuproine Cu(I) complex **C5** (Figure S7).[9] One notices that the MLCT bands are more intense as well, because of the increased ground state dipolar moment generated by the combination of electron poor $\mathbf{L^0}$ and electron rich $\mathbf{L^n}$. The complexes **C3** and **C4** present higher light harvesting efficiency in the visible than **C1** and **C2** because of an intense additional intraligand charge transfer transition (ILCT), located at the edge of the visible around 420 nm.[9]

	λ (nm) [ε ($M^{-1}.cm^{-1}$)]	E (V)* [ΔE (mV)]	
C1	477 [$4.7\cdot10^3$]	0.94 [96]	–
C2	500 [$9.8\cdot10^3$]	0.91 [96]	–
C3	504 [$1.3\cdot10^4$]	1.08[a] [-]	0.80[a] [-]
C4	502 [$1.4\cdot10^4$]	1.03[b] [-]	0.95[b] [-]

Table 1. UV-Visible and electrochemical data for **C1-4**. *data collected with the methyl ester forms of **C1-4**.

This very intense ILCT transition corresponds to a shift of the electron density from the electron rich amine moieties to the electron poor pyridine. Such band does exist for **C2** too, but is significantly blue-shifted compared to **C3** and **C4** because of the poorer electron donating power of $\mathbf{L^2}$. Spectra recorded on TiO_2 transparent electrodes (Figure S3) feature the same patterns than those recorded in solution phase (Figure 2). Overall, the complexes displayed a rather broad and intense absorption over a large wavelength frame (λ_{onset}~620 nm), revealing their potentials

as wide band gap semi-conductors sensitizers.

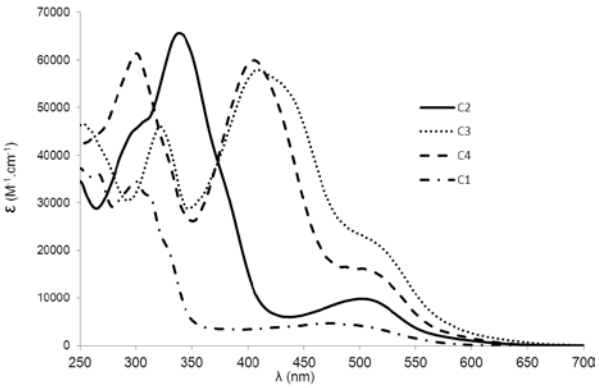

Figure 2. UV-Visible spectra of complexes **C1** (dash-dot), **C2** (plain), **C3** (dot) and **C4** (dash) recorded in dichloromethane.

No luminescence was detected upon excitation in the MLCT band, regardless the conditions. This could be due to *cis-trans* isomerization of the vinyl double bond[12] or the lesser rigidity of the Cu-bpy coordination cage compared to Cu-Phen, facilitating the deleterious exciplex quenching.

To record better resolved cyclic and pulsed voltammograms (no adsorption of the dye on the electrode), these measurements were performed on the diester forms of complexes. The latter featured the expected, reversible copper-centred oxidation around 1 V vs. SCE (Table 1). The voltammograms of **C3ester** and **C4ester** displayed an additional oxidation wave at 0.95 and 0.80 V vs. SCE respectively, corresponding to the removal of one electron from the NR_2 (R = ethyl or phenyl) amine moieties. Only differential pulse voltammetry allowed discriminating the two close oxidation steps for complex **C4ester**. The higher Cu^{II}/Cu^{I} potentials displayed by **C3ester** and **C4ester** likely originate in the coulombic repulsion between the copper cation and the electrogenerated hole on the amine fragment.

The combination of electrochemical and UV-Vis data allowed evaluating the Gibbs energies associated to the various charge transfer processes. In all cases, both charge injection and dye regeneration are exergonic (ca. 300 meV, see Table S1 in SI). Energy-wise, **C1**-**4** feature roughly the same behaviours. TiO_2 electrodes were dipped while still hot for two days in ethanolic solutions of **C1**-**4** and the photovoltaic devices were then assembled with a platinum counter-electrode, sealed with a hotmelt polymer frame and their performances along those of the reference benchmark **N719** were evaluated under AM 1.5 calibrated artificial sunlight (Table 2 and SI for details).

	Voc (mV)	Jsc (mA.cm^{-2})	FF (%)	PCE (%)
C1[a]	475	2.20	72.80	0.76
C2[a]	535	2.89	72.54	1.12
C3[a]	545	7.51	71.52	2.93
C4[a]	565	6.70	73.32	2.77
N719	635	16.87	68.69	7.36
C1[b]	525	3.76	74.64	1.47
C2[b]	565	4.99	72.39	2.04
C3[b]	605	10.86	70.97	**4.66**
C4[b]	625	10.13	69.76	4.42

Table 2. Photovoltaic data for DSCs based on TiO_2 sensitization by **C1**-**4** without (a) and with (b) **CDCA**. Voc: open circuit voltage; Jsc: short circuit current density; ff= fill factor.

The weakest PCE is afforded by **C1** based DSCs, grounded in low photocurrent and photovoltage. The latter is assigned to a lower light harvesting efficiency (LHE) and probably to an exacerbated charge recombination with the electrolyte. Indeed, the positive charge of **C1**-**4** entails a coulombic repulsion between them on the surface of TiO_2, increasing the number of unoccupied adsorption sites and thus recombination centres. **C3**, **C4** and **C2** are a lot bulkier than **C1**, and thus passivate more the surface of the semi-conductor, yielding a higher Voc. This is further confirmed by the higher dark current displayed by **C1**-based DSCs (see SI). Besides, both **C1** and **C2** yield poor photocurrents, likely because of their less intense absorption coverages of the solar spectrum, leading to an overall weaker LHE (see Figures 3& S4).

The short circuit currents of **C3** and **C4** based DSCs are by far the highest of the series, in part because of the presence of ILCT bands in the visible domain, increasing the LHE. This is confirmed by the incident photon to current efficiency (IPCE) recorded on each DSC, where a current generation is indeed monitored between 400 and 460 nm for **C3** and **C4** (around 43% at 410 nm). **C1** and **C2** based DSCs, being deprived of such ILCT above 400 nm consequently display lesser LHE and IPCE.

Spin coating a 0.1M **CDCA** (chenodeoxycholic acid) ethanolic solution onto the photo-electrodes prior to the final sealing is anticipated to eliminate the deleterious self-quenching process induced by aggregation. Rewardingly, unprecedented improvements in the power conversion efficiencies (PCEs) of all DSCs were observed upon such **CDCA**-surface treatment. First of all, an increase of the photopotential was observed for all DSCs. **C1**-**4** based devices exhibited a 50-60 mV rise of the Voc, together with a decrease of the dark current. This improvement was therefore assigned to the higher electron concentration in the CB and to a passivation of recombination sites by the co-adsorbent molecules. In the case of **C2**, the octyl chains may provide a built-in, efficient protection of titanium dioxide's surface, thus explaining the lesser increase of the Voc (ca. 30 mV). The electron lifetime (τ_n) and mean transit time (τ_{tr}) of photoinjected charge carriers were then recorded by intensity-modulated photovoltage spectroscopy (IMVS) and intensity-modulated photocurrent spectroscopy (IMPS). However, these measurements reveal that no significant improvement of both τ_n and τ_d was observed when **CDCA** was added in the preparation of the series of solar cells (see SI). As a result, the charge collection efficiency η_{coll} measured as a function of the illumination intensity is quite similar for all the dyes (see SI).

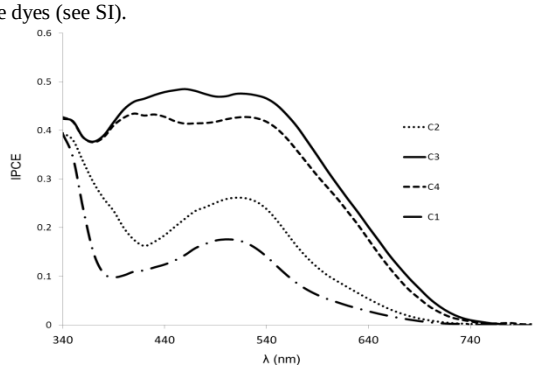

Figure 3. IPCE for DSCs sensitized with **C1** (dash-dot), **C2** (dot), **C3** (plain), and **C4** (dash) recorded with **CDCA**.

The most spectacular improvement of the PCE originates in the rise of

the Jsc for all devices. One calculates a 70% increase of the photocurrent for **C1** and **C4** and 45 and 50% for **C2** and **C3** based photovoltaic devices, respectively. For a better understanding, IPCEs of DSCs with and without **CDCA** treatment were compared (Figure S5). A significant increase of the IPCE is observed for **CDCA**–treated cells, regardless the dye (Figure 3), together with a broadening of the signals. Several reasons can be invoked to rationalize this important result. First, **CDCA** molecules release protons and this bends the conduction band downwards, increasing thus the driving force of the electron injection into the semi-conductor, and consequently improving the electron injection yield.[13] Second, a noticeable increase of the absorbance of **C1**-**4** based photo-electrodes was monitored upon **CDCA** treatment, along with a slightly broadened MLCT transition (Figure S4). These subtle changes in the absorption spectra of the chemisorbed complexes are in line with the IPCE, and are probably grounded in a reorganization of the dye monolayer upon **CDCA** adsorption. The role of **CDCA** is often associated with the disruption of dye aggregates and certainly comes into play here, especially due to the presence of organic styryl branches on the complexes **C2**-**4**. Based on the effect of **CDCA** on both IPCE measurements and on the Jsc enhancement, we conclude that the main role of **CDCA** with these complexes is certainly to decrease the aggregation on TiO_2 surface leading to higher LHE and injection quantum yield. In these conditions, DSCs provided a maximum PCE of 4.66% for **C3**-based device. This is to date the highest PCE ever reported for a DSC based on a copper(I) complex sensitizer, and hold great promises for the future of these cheap solar cells. Most highly performing dyes, including ruthenium complexes, are neutral species, while these first series of copper(I) complexes are positively charged. This is certainly one weak point of these dyes, which can be overcome by using new ancillary ligands

Conclusions

We successfully isolated four stable heteroleptic copper(I)-polypyridine complexes, using the HETPHEN concept. Through a careful choice of ligands, unprecedented PCE were measured, reaching 4.66%. The new anchoring ligand $\mathbf{L^0}$ paves the route to prepare other sensitizers as it certainly forms stable heteroleptic copper(I) with many unhindered diimine ligands. This contribution brings further credit to these molecular complexes as efficient sensitizers for DSCs, *en route* for a cheap and less toxic substitute to ruthenium dyes.

Acknowledgements

ANR agency is gratefully acknowledged for the financial support of these researches through program HeteroCop (n° ANR-09-BLAN-0183-01).

Notes and references

[a] *UNAM, Université Nantes, Angers, Le Mans, CEISAM, Chimie Et Interdisciplinarité, Synthèse, Analyse, Modélisation CNRS, UMR CNRS 6230, 2, rue de la Houssinière - BP 92208; 44322 NANTES Cedex 3 (France) E-mail: Fabrice.Odobel@univ-nantes.fr and Mohammed.Boujtita@univ-nantes.fr*

[b] *UMR CNRS 6226-Université de Rennes 1, Sciences Chimiques de Rennes, Campus de Beaulieu, 35042 Rennes Cedex, France. .*

[c] *Current address: CEMCA UMR CNRS 6521, Université de Bretagne Occidentale, 6 avenue Victor Le Gorgeu, 29238 Brest, France*

† Electronic Supplementary Information (ESI) available: Synthesis of the complexes, absorption spectra on TiO_2 and electron lifetime (τ_n), mean electron transit time (τ_{tr}) and η_{coll} measured by IMVS and IMPS. See DOI: 10.1039/b000000x/

1. O'Regan, B.; Gratzel, M., *Nature* **1991,** *353* (6346), 737-740.
2. Hagfeldt, A.; Boschloo, G.; Sun, L.; Kloo, L.; Pettersson, H., *Chem. Rev.* **2010,** *110* (11), 6595-6663.
3. Mishra, A.; Fischer, M. K. R.; Bauerle, P., *Angew. Chem., Int. Ed.* **2009,** *48*, 2474-2499.
4. Sakaki, S.; Kuroki, T.; Hamada, T., *Dalton Trans.* **2002,** (6), 840-842.
5. Bozic-Weber, B.; Constable, E. C.; Furer, S. O.; Housecroft, C. E.; Troxler, L. J.; Zampese, J. A., *Chem. Commun.* **2013,** *49* (65), 7222-7224.
6. Bozic-Weber, B.; Constable, E. C.; Housecroft, C. E., *Coord. Chem. Rev.* **2013,** *257* (21–22), 3089-3106.
7. Pellegrin, Y.; Sandroni, M.; Blart, E.; Planchat, A.; Evain, M.; Bera, N. C.; Kayanuma, M.; Sliwa, M.; Rebarz, M.; Poizat, O.; Daniel, C.; Odobel, F., *Inorg. Chem.* **2011,** *50* (22), 11309-11322.
8. Sandroni, M.; Kayanuma, M.; Planchat, A.; Szuwarski, N.; Blart, E.; Pellegrin, Y.; Daniel, C.; Boujtita, M.; Odobel, F., *Dalton Trans.* **2013,** *42* (30), 10818-10827.
9. Sandroni, M.; Kayanuma, M.; Rebarz, M.; Huriye, A.-K.; Pellegrin, Y.; Blart, E.; Poizat, O.; Le Bozec, H.; Sliwa, M.; Daniel, C.; Odobel, F., *Dalton Trans.* **2013,** *42*, 10818-10827.
10. Schmittel, M.; Ganz, A., *Chem. Commun.* **1997,** (11), 999-1000.
11. Armaroli, N.; Accorsi, G.; Cardinali, F.; Listorti, A., *Top. Curr. Chem.* **2007,** *280* (Photochemistry and Photophysics of Coordination Compounds I), 69-115.
12. Aubert, V.; Ordronneau, L.; Escadeillas, M.; Williams, J. A. G.; Boucekkine, A.; Coulaud, E.; Dragonetti, C.; Righetto, S.; Roberto, D.; Ugo, R.; Valore, A.; Singh, A.; Zyss, J.; Ledoux-Rak, I.; Le Bozec, H.; Guerchais, V., *Inorg. Chem.* **2011,** *50* (11), 5027-5038.
13. Nazeeruddin, M. K.; Humphry-Baker, R.; Liska, P.; Grätzel, M., *J. Phys. Chem. B* **2003,** *107* (34), 8981-8987.

Graphical abstract for entry